Journal of Undergraduate Chemistry Research, **2022**,21(2), 33

SPATIAL AND VEGETATIONAL EFFECTS ON CARBON DYNAMICS IN SALT MARSH SOILS

Abigail A. Whittington*, Rachel Owrutsky†, Andrew Wozniak†

* Chemistry Department, Vassar College, 124 Raymond Avenue, Poughkeepsie, NY 12604.
† School of Marine Science and Policy, College of Earth, Ocean, and Environment, University of Delaware, Lewes, DE 19958.

Abstract

Salt marshes are important for long-term storage of carbon (C). How C sequestration in marshes varies spatially due to vegetational coverage and proximity to tidal creeks is unclear. Dissolved and particulate organic C (DOC + POC) pools were examined in salt marsh cores from the Great Marsh, DE . Two vegetated and two unvegetated 1-meter cores, defined as being close (15 m) and far (100 m) from the tidal creek were processed for POC and DOC quantities, fluorescent DOC, and base extractable POC characteristics (via Excitation Emission Matrix Spectroscopy). The marsh OC pools exhibited large shifts in quantities and characteristics, even on spatial scales less than 10 m, with distance from the tidal creek having a greater impact than the vegetation at the marsh surface. Findings indicate differences in OC with depth, distance from the tidal creek, and for POC versus DOC. The data presented may indicate that heavier, more complex forms of C are sequestered long-term.

†Corresponding authors: rjowruts@udel.edu, awozniak@udel.edu
Keywords: salt marsh, blue carbon, fluorescence spectroscopy, organic carbon

Introduction

Salt marshes sequester blue carbon (C), or C stored in the sediments of coastal ecosystems, at relatively high rates (218 ± 24 g C m^2/year), similar to seagrass and mangrove environments[1]. As climate warms and sea-levels rise, a critical point is reached when sections of marshes will drown, and no more C will accumulate, making marsh protection essential in climate change policies[2]. With anthropogenic activities encroaching on the upland edges of salt marshes, many marshes cannot migrate landward to replace the C sink. Given the wide range of blue C flux estimates,[1] it is clear that C is sequestered at different rates spatially, but the mechanisms driving that spatial variability are not fully understood. Understanding this variability may provide land managers guidance in terms of which marsh environments to protect in order to maximize the retention of blue C.

To understand blue C sequestration, we must delve into the sources and sinks of organic C (OC) in salt marshes. Salt marsh OC is produced by salt marsh plants and brought to marsh soils with freshwater and marine/estuarine waters. C exits marshes through both lateral movement and conversion to inorganic compounds, which can be transported laterally to estuarine creeks or vertically to the atmosphere[3]. Vertical movement occurs when OC breaks down via microbial respiration processes to inorganic components, such as CO_2 or CH_4 gas, which can move to the atmosphere. Lateral movement occurs when pools of dissolved organic carbon and/or inorganic gasses within the marsh follow hydrological pathways to the tidal creek, a process known as tidal flushing. Tidal flushing can also remove solubilized particulate organic C. The particulate organic C that resists degradation and transport is left behind in the sediments and can be sequestered on decadal or longer timescales.

The susceptibility of salt marsh soil OC to be lost by these various processes can vary depending on its local biogeochemical environment and molecular composition. The presence, species, and phenological phase (stage within the annual cycle of plant growth from Greenup to Maturity to Senescence to Dormancy) of plants influence C dynamics. Methane and carbon dioxide emissions from the St. Jones Marsh, in Delaware, for example, vary across growing phases of *Spartina alterniflora* and have been shown to vary spatially.[3] Carbon emissions vary on regional and local (e.g., within a marsh) scales[4,5]. In addition, marshes have different plant types, which contribute different OC due to unique biochemistries.

The hydrology of marshes affects how C is held in sediments and how porewaters, the water held in spaces between soil and sediment particles, are flushed. Regions on the interior of a marsh with higher elevations have less frequent tidal flushing, giving C a chance to persist long enough to be converted into recalcitrant compounds that can be sequestered. Sediment accumulation rates may be significant in long-term C sequestration, as they deposit carbon-bearing compounds that have potential for sequestration[6]. Soils in the Canary Creek marsh area near the coring site used in this study accumulate at a rate of 0.29 ± 0.18 cm/year[6]. Salt marsh soil geochemistry and vegetation may also affect C storage by providing an environment that facilitates degradation or mineral complexation. For example, Fe has been shown to form complexes with organic matter that may immobilize organic compounds[7]. Fe concentration and species in a marsh varies depending on tide stage, salinity, and location[8]. Therefore, Fe complexing may also vary with tide, salinity, and location.

There are many factors affecting C storage within salt marshes, many of which are spatial controls, including salinity, biogeochemical factors, wetland type, and latitudinal gradients[9,10]. Recently mid infrared spectroscopy and partial least squares regressions have been used to accurately estimate the OC of marshes[11]. Despite the progress in measuring and estimating OC, it is imperative to collect and analyze samples to allow for increased confidence in models. Sampling could be standardized once there is a greater understanding of how C is sequestered, streamlining marsh research and improving models.

The overarching questions that informed this study are: why does C remain in the marsh and what are the primary controls on this storage? To begin answering these questions, we chose to analyze the effect of vegetation and spatial variability on C from cores collected within the Great Marsh, located in Lewes, DE. Through the analysis of total organic carbon in both porewaters and sediments, as well as an in-depth examination of the fluorescence and absorbance of the dissolved and base-extractable organic matter, we were able to evaluate depth profiles of C characteristics at vegetated and unvegetated sites close and far from the tidal creek. It is important to note that each site was analyzed using only one core, limiting our ability to extend the results of the study to the scale of the entire marsh. Despite this limitation, these data will add to the body of knowledge informing our understanding on how C moves and is stored in marshes. Understanding loss and storage processes will enhance how we value marsh environments and their roles in C sequestration.

Methods

Location and Conditions of Coring

Delaware has 308 km^2 of tidal marshes along the western shore of the Delaware Estuary[12] making it an ideal location to study the sequestration of blue C. In these wetlands, C accumulates at an estimated rate of 172.4 ± 85.9 g C m^2/year[6]. Delaware marshes prove useful in studying blue C and its effects on the rapidly changing climate, specifically for the mid-Atlantic region of the United States.

Figure 1: Coring sites: (a.) Unvegetated close, (b.) vegetated close, (c.) unvegetated far, (d.) vegetated far. (e.) RTK GPS of the coring site in Lewes, DE.

Cores were collected from the Great Marsh in Lewes, Delaware on June 23, 2021. Cores were collected at mid to low falling tidal ranges using 1 m clear PVC coring tubes with a 5.7 cm diameter. Four cores were collected in total, two located within approximately 15 m of the tidal creek and two located within 100 m of the tidal creek (Figure 1). In each location, one core was collected from a vegetated spot while the other was collected in an unvegetated spot (Figure 1). These cores are hereafter referred to as VC (vegetated close), UVC (unvegetated close), VF (vegetated far), and UVF (unvegetated far).

Coring and Sectioning Procedures

Cores were collected by hammering the clear plastic coring tube into the ground. The distances from the top of the core on the interior of the tube to the marsh surface on the exterior of the tube were measured. The difference in these two lengths was used to establish how much each core had compacted. Core tubes were removed from the marsh and both the top and bottom of the tube were capped immediately to prevent oxidation. In the laboratory, the cores were extruded from their clear tubes and sectioned using a serrated knife inside of a N_2-filled glove bag to maintain anoxia. Five desired sections with the same true depth were calculated using compaction measurements. Three-cm sections were placed into three labeled 50-mL centrifuge tubes and refrigerated until porewater extraction could be performed (< 24 hours).

Section Processing Procedures

To extract porewater, the 50-mL tubes containing core sections were centrifuged for 30 minutes. In an anoxic glove bag, the porewater, now sitting above the soil, was pipetted into a 10-mL syringe attached to a 0.2 µm Teflon filter. The porewater was syringe-filtered into a labeled vial that had been purged with N_2 gas. The porewaters and sediments were refrigerated until analysis. Each section was placed into a foil boat and dried in an oven (55°C). Sediment was then ground up with a glass pestle. The sediment was shaken through a 4-mm sieve to remove roots. Ground sediments were homogenized using a coffee grinder and then transferred to glass jars using a clean glass funnel. These jars were stored in the freezer until analysis.

Porewater Procedures

Before analysis, porewaters were removed from the refrigerator and allowed to come to room temperature.

Iron Analysis

Argon gas was bubbled through house deionized water for 30 minutes before making iron standards. Ferrous ammonium sulfate standards (0.005 M) were made in a deoxygenated environment. The iron standard curve (6 points) ranged from 0.00 M to 28.76 µM after the addition of ammonium acetate (NH_4Ac) and ferrozine. Iron standards were analyzed on the Horiba Aqualog® (USA) at 562 nm. Samples for iron analysis had 100 or 400 µL of porewater added (determined by quantity available) to 1800 µL DI water, 200 µL 2.5 M NH_4Ac, and 20 µL 0.01 M ferrozine. Samples were analyzed at 562 and 230 nm. The cuvette was rinsed with ultrapure MilliQ water between every sample.

Total Organic Carbon Analysis

Dissolved organic carbon (DOC) concentrations were mea-

sured using the established high temperature catalytic oxidation method using a Total Organic Carbon Analyzer (TOC-V CPH, Shimadzu, USA) operated in the non-purgeable organic carbon mode[13,14]. The instrument was operated at 680°C, with a five-point calibration curve using potassium hydrogen phthalate as a carbon standard. Certified reference materials of deep seawater (40-44 µM DOC) obtained from the Hansell Lab at the University of Miami were used to verify instrument performance. Samples were acidified to a pH of ~2-3 using 2 M HCl to remove any inorganic carbon during the purging step. Blank contributions to the DOC values were assessed using low DOC Milli-Q added to the sample bottles that were then stored and processed in the same manner as samples. Blank contributions were minor and subtracted from sample values.

Excitation Emission Matrix Spectroscopy (EEMs) Analysis

The absorbance spectrum of the chromophoric dissolved organic matter (CDOM) was obtained between the wavelengths of 230 nm and 700 nm using a Horiba Aqualog® with a pathlength of 1 cm. Fluorescent excitation emission matrix spectroscopy (EEMs) was performed over an excitation/emission (ex/em) range of 230-700 nm/245-822 nm using a Horiba Aqualog®. If the absorbance at $\lambda = 254$ nm was above 0.2, the sample was diluted prior to EEMs analysis to avoid saturating the fluorescence detector. Each EEM was subjected to an inner filter effect correction using absorbance data collected as described[15]. Spectra were also Raman calibrated[16]. The humification index (HIX), biological index (BIX), and fluorescence index (FI) were calculated using the eemR package in R[17].

Sediment Analysis Procedures

Base Extraction of Sediment Particulates

The operationally-defined particulate organic carbon (POC) pool (does not pass through a 0.7 µm filter after extraction with water) is partially fluorophoric[18] allowing it to be analyzed using techniques most commonly used for dissolved components after extraction with base. Sediments were removed from the freezer before extracting into a liquid phase using sodium hydroxide. 0.1 M NaOH was prepared, sonicated for 15 minutes, and degassed with N_2 gas for 30 minutes. One g of sediment was placed in a 50-mL centrifuge tube with 40 mL 0.1 M NaOH and capped with N_2 gas to maintain anoxia. The mixture was shaken at 150 rotations per minute on a shaker table for 24 hours. After shaking, the mixture was centrifuged for 15 minutes and decanted into a labeled 250 mL bottle, which was filled with N_2 gas prior to capping. Another 40 mL of base were added to the remaining solids, and the previous steps of filling with N_2 gas, shaking, centrifuging, and decanting were repeated two more times. After the third repetition, 30 mL of Milli-Q water was added to each 50-mL tube and the tubes were shaken to obtain a neat suspension. Then, the tubes were centrifuged for 5-8 minutes and decanted into 250-mL bottles. The bottles were capped with N_2 gas and stored in the refrigerator until syringe filtering. Directly prior to filtering, the base extract bottles were shaken for optimal mixing. About 5 mL of base extract were poured into a 10 mL syringe with 0.22 or 0.45 µm Teflon filters. The extract was filtered into small 20 mL vials, which were capped with N_2 and stored in the refrigerator at 4°C.

Total Organic Carbon and EEMs Analyses

Base extracts were analyzed for TOC and EEMs following the same methods described for the dissolved porewaters.

Total Iron Analysis

The Fe (III) in the filtered base extracts was converted to Fe (II) for analysis by mixing 1.8 mL of DI water, 0.2 mL of 2.5 M NH_4Ac, and 20 µL of 0.1 M HCl-hydroxylamine with 600 µL of sample[19]. Samples were covered in foil for 24 hours. House DI water was bubbled with Ar for 30 minutes. A 0.005 M iron standard was prepared using ferrous ammonium sulfate. The iron standard curve (6 points) ranged from 0.00 M to 28.76 µM after the addition of NH4Ac and ferrozine. Iron standards were analyzed on a UV/VIS Spectrometer at 562 nm. Samples had 100 µL of ferrozine added and were analyzed on the UV/VIS Spectrometer at 562 nm.

Results and Discussion

Spatial versus Vegetational Variability

Figure 2 shows depth profiles for porewater DOC concentrations in the vegetated and unvegetated cores. Both the unvegetated and vegetated cores from the site close to the tidal creek follow a similar trend of decreasing from 2 cm to 11 cm, with a gradual increase to 44 cm suggesting that surface vegetation does not affect DOC close to the tidal creek. The unvegetated and vegetated cores farther from the creek have very different DOC concentrations near the marsh surface with the unvegetated core (DOC = 2737 µM) having a lower concentration of DOC than the vegetated far core (DOC = 5042 µM). This is indicative of a vegetational influence for surface DOC farther away from the creek. At the greater depths sampled, these two sites have similar, increasing concentrations suggesting any vegetational influence on DOC may be confined to the surface of the core. Interestingly, all four cores appeared to have similar concentrations at a depth of ~ 17 cm, an area where root biomass was observed to be abundant, with DOC ranging between 2780 and 3665 µM. At every depth measured, DOC concentrations were higher at the site farther from the tidal creek (Figure 2). This may be indicative of longer residence times and slower removal rates for DOC in this region of the marsh from less frequent tidal flushing[20,21].

Depth profiles of the base-extractable organic carbon concentrations at each coring site (Figure 3) show little difference due to

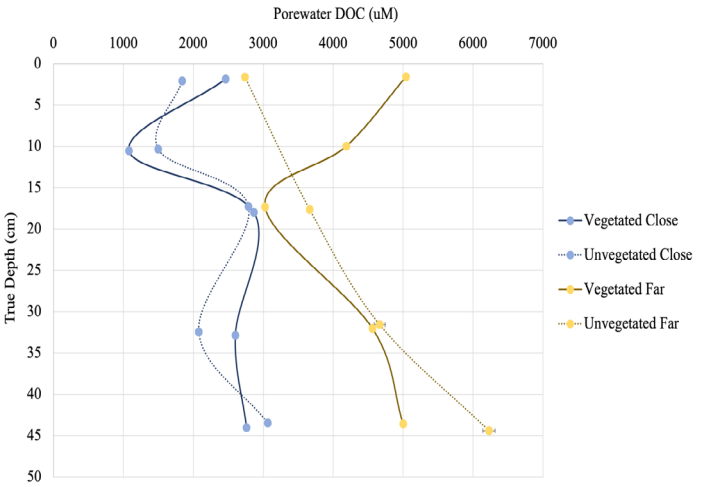

Figure 2: Porewater DOC concentrations plotted against the depth of sample collection for the vegetated and unvegetated cores collected close to and farther from the tidal creek.

vegetative cover but considerable differences related to distance from the tidal creek. In the site closer to the tidal creek, the unvegetated and vegetated cores measure similar concentrations of BEPOC across all depths sampled. UVC and VC showed an increase in C concentration with depth with a range of 7.0 mg C/g sample at 2 cm to 11.9 mg C/g sample at 44 cm suggesting BEPOC becomes more concentrated with depth. BEPOC increased slightly in UVF and VF cores from the surface (2 cm = 18 mg C/g sample) to above the root area (11 cm = 21 mg C/g sample) and then decreased until 44 cm (2.5 mg C/g sample). There are no major discrepancies in the BEPOC between UVF and VF at the surface. They follow similar trends with depth except for around 17 cm, where UVF had 19.0 mg C/g sample and VF had 11.9 mg C/g sample. As was observed for all 4 cores for porewater DOC, 3 of the 4 cores show BEPOC concentrations that converge (8.8 - 11.9 mg C/g sample) near the root zone at ~17 cm depth suggesting that OC processes at these root zone areas are relatively consistent regardless of vegetational cover or distance from tidal creek.

At any given point within a core, the C present is a sum of different inputs and outputs. Cores taken from the site farther from the tidal creek show higher concentrations of carbon near the soil surface because this region is subject to a less dynamic hydrological regime. Only the highest of incoming tides flood these areas bringing oxygen for aerobic microbial processes and removing any DOC that accumulates since the last flushing event. Cores taken closer to the tidal creek have more C inputs than outputs at depth from hydrological transfers due to remineralization and lateral transport. Hydrological flow may be bringing C from the surface of the marsh interior to deep parts of the marsh near the creek, which would mask some of the diagenetic C losses.

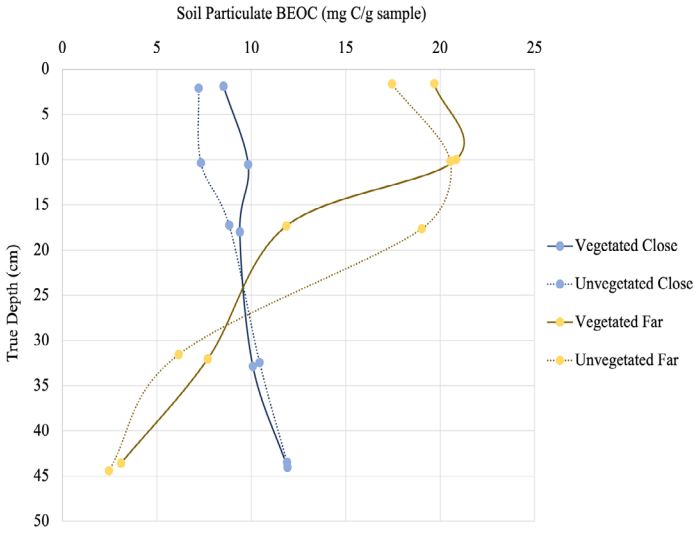

Figure 3: Base extractable particulate organic carbon (BEPOC) concentrations plotted against the depth of sample collection for the vegetated and unvegetated cores collected close to and farther from the tidal creek.

This data comparison suggests that hydrological variability (i.e., distance from a tidal creek) could be more important for controlling carbon concentrations in a marsh than the presence or absence of vegetation. This may be, in part, due to the fact that the presence of vegetation at the marsh surface is not always indicative of past vegetative conditions or because the lack of vegetation does not preclude the presence of roots below an unvegetated location. In fact, evidence for the presence of a root network underneath the surface of the marsh was observed for all four cores. Belowground root density appears to cause a more uniform spread of organic carbon than surface vegetation indicates, as aboveground vegetation has little effect on C concentration past 10 cm. Roots change the oxygen content of the soil, causing different microbes to be present. There appears to be a different biogeochemical zonation with and without roots, which could be controlled by the different types of microbial species available.

Iron Analysis

Figure 4 presents iron concentration data in the dissolved and base extracted solid phase of the core sections. These data demonstrate that each core has a unique redox environment, controlled by the availability of favorable oxidants and determines the thermodynamics of organic matter decomposition[22]. Iron is known to interact with marsh sediments, at times resulting in the formation of pyrite and iron sulfides.[22] During the summer, surface oxidation of iron is most common, resulting in plant growth stimulation and the sustenance of an active microbial community.[23] Plants are available to create organic ligands, which enable the reduction of Fe(III) to Fe(II). Fe(II) is readily oxidized while in organic chelates by Fe(III) minerals as part of the redox cycle.[24] The essential aspect of this marsh redox system is the ability of iron to bind to

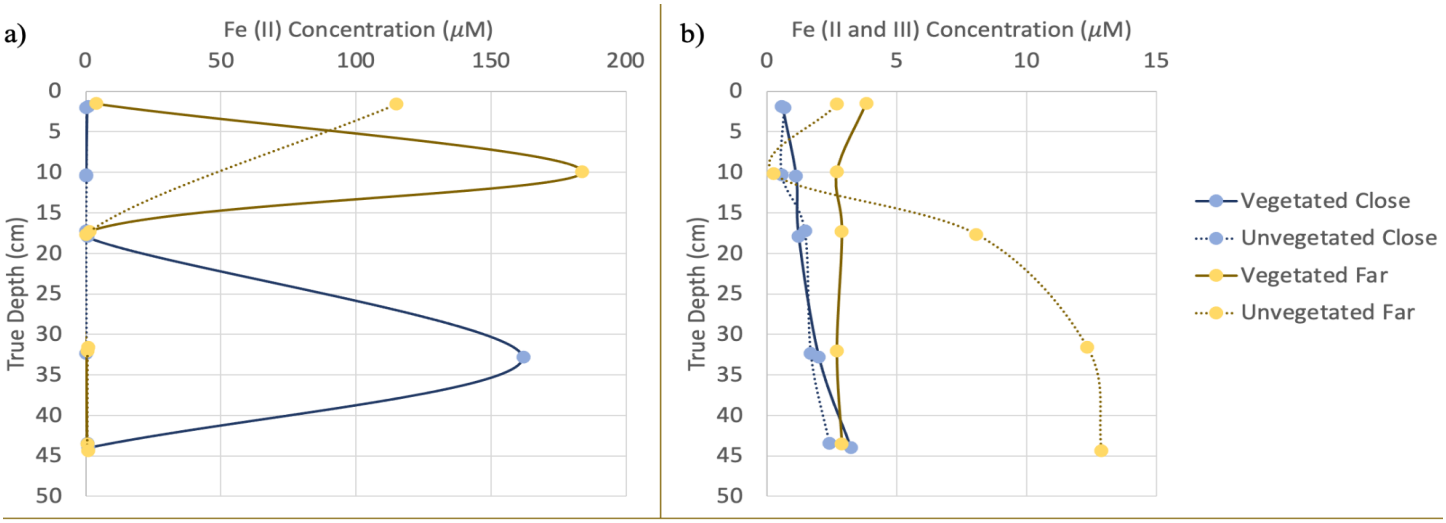

Figure 4: Depth profile for a) Fe(II) in porewater (dissolved phase) and b) Fe(II) and Fe(III) in base extracts of particulate organic carbon. No data for UVF-10cm due to insufficient porewater.

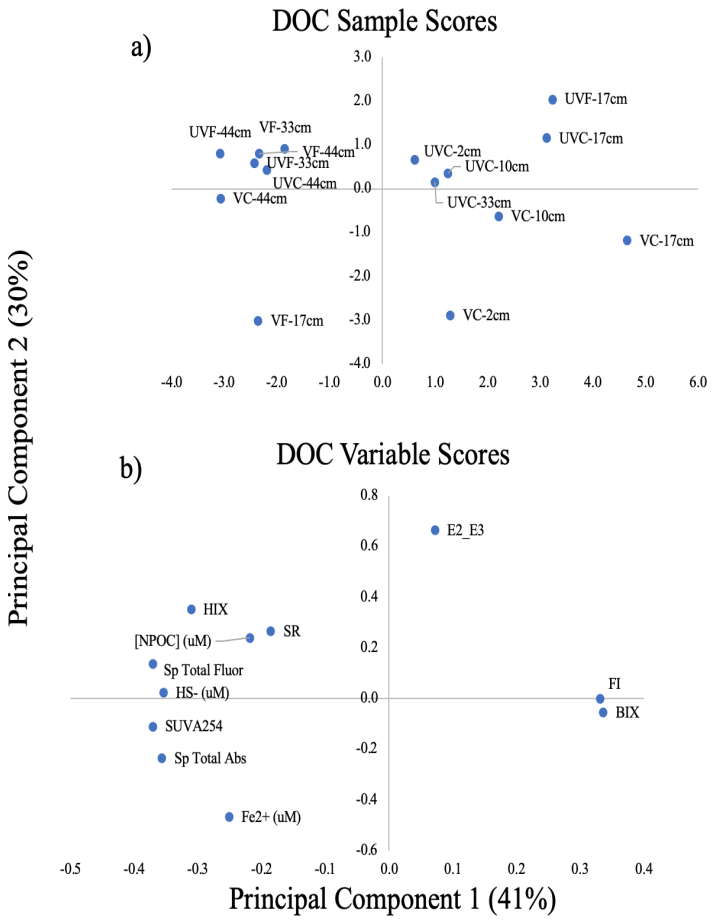

Figure 5: Principal component analysis a) sample scores and b) variable loadings for principal components 1 and 2 from analyses performed on porewater dissolved samples.

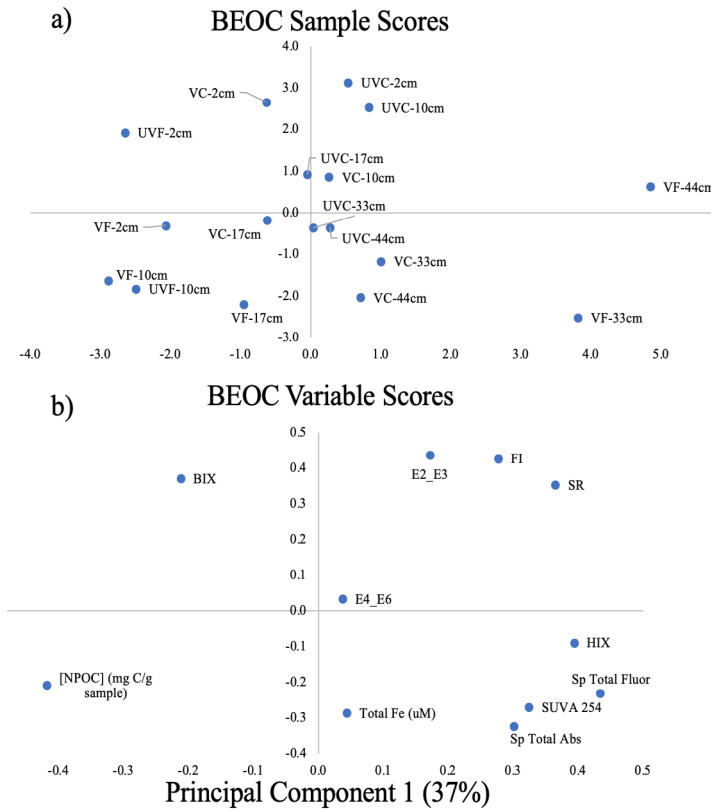

Figure 6: Principal component analysis a) sample scores and b) variable loadings for principal components 1 and 2 from analyses performed on base extracts of the particulate samples.

organic materials which creates a complex that is important within the context of this experiment.

In the porewater of VC-33cm, VF-10cm, and UVF-2cm, where Fe concentrations are elevated, we may expect to observe fluorescence quenching in the associated EEMs. Base-extracted sediment of UVF-17cm, UVF-33cm, and UVF-45cm contain high Fe concentrations, possibly causing quenching in the EEMs spectra. Iron participates in static quenching, in which the metal forms a complex with DOM that does not fluoresce with the same intensity[25,26,27]. Both Fe^{3+} and Fe^{2+} alter intensities of fluorescence and peak positions observed for humic (dense organic compounds related to humus) fluorophores[28].

Impact of Depth on DOC and BEPOC Fluorescence

All dissolved and base-extracted samples contained abundant fluorescent organic material. The analysis of various metrics and indices calculated from the data showed that samples with higher Fe concentrations also had characteristics consistent with quenching, in which signals were decreased from their expected values.

Table 1: Biological indices (BIX) and humification indices (HIX) data for porewater (dissolved phase) and base extracts of particulate organic carbon. No DOC data for UVF-10cm due to insufficient porewater.

Sample ID	DOC BIX	DOC HIX	BEPOC BIX	BEPOC HIX
VC - 2cm	0.69	5.14	1.09	7.38
VC - 10cm	0.71	2.76	1.04	8.76
VC - 17cm	0.86	1.92	0.98	9.67
VC - 33cm	0.68	7.81	1.05	11.9
VC - 44cm	0.58	14.9	0.90	10.3
UVC - 2cm	0.68	12.3	1.11	8.60
UVC - 10cm	0.68	12.5	1.14	8.92
UVC - 17cm	0.70	5.64	1.04	9.20
UVC - 33cm	0.68	10.6	1.03	11.4
UVC - 44cm	0.59	14.7	0.99	9.99
VF - 2cm	1.11	1.49	1.03	6.44
VF - 10cm	0.90	2.25	1.01	8.58
VF - 17cm	0.64	7.22	0.89	8.99
VF - 33cm	0.61	15.5	0.75	11.4
VF - 44cm	0.61	17.2	0.74	19.2
UVF - 2cm	0.82	4.07	1.04	8.02
UVF - 10cm			0.80	8.66
UVF - 17cm	0.75	8.00	0.95	6.12
UVF - 33cm	0.66	13.2	0.76	4.57
UVF - 44cm	0.67	14.1	0.86	4.01

Figures 5 and 6 present statistical analyses of all the data that were not impacted by iron quenching. An initial principal component analysis run for EEMs and organic carbon measurements for a combined DOC and BEPOC sample dataset showed sample scores separated based on whether the analyses were run on the base extract or the porewater DOC (data not shown). This demonstrated expected fundamental DOC compositional differences that relate to DOC compound solubility. When these pools were compared separately, they demonstrated similar controlling variables for the fluorescent BEPOC and DOC compositions. Shallow sampling depths have higher values of BIX, a biological index calculated using EEMs data (Table 1). BIX typically increases with marine humic influence and fresh biological activity/production[29]. As the BIX values decrease with depth, the data demonstrated higher levels of terrestrial influence and less microbial activity with depth in a core. Shallow depths of the marsh have the highest biological production and more marine influence. With depth, degradative processes remove the most labile, biologically-sourced materials leaving behind organic materials that have been transformed, or humified, losing this biological signature.

Greater sampling depths for all cores and both carbon pools (dissolved and base extracts) aligned strongly with higher HIX and $SUVA_{254}$ values (Table 1). HIX indicates how humified a sample is[30]. Humified materials are typically described as high molecular weight, organic compounds that result from a series of diagenetic transformations of biologically-sourced compounds. HIX values above 10 often align with highly humified, terrestrial organic material with high levels of aromaticity and high molecular weights[31]. Below 30 cm, sediments had higher HIX values, pointing to an increase in humified material with large, aromatic molecules at the deeper depths sampled. When UV absorption at 254 nm is normalized to the concentration of DOC, it results in $SUVA_{254}$. This measurement correlates strongly with aromaticity for many isolated humic substances[32]. The apparent high correlation between these deeper samples in the marsh and the $SUVA_{254}$ and HIX metrics presents strong evidence for the presence of humified, aromatic molecules at depth in the marsh. These high molecular weight compounds may be further transformed by abiotic and biotic diagenetic processes over time. The high HIX and $SUVA_{254}$ values at this depth are consistent with these humified and aromatic compounds being harder to break down and suggests they make up a considerable portion of the sequestered blue carbon in these systems.

Conclusions

Variations in salt marsh organic matter quantities and characteristics appear to be more impacted by distance from the tidal creek than the presence or absence of vegetation on the surface of the marsh. Marsh environments also show high biogeochemical variability within local regions of the salt marsh, as evidenced by the large fluctuations in iron concentrations for sites within 10 feet of each other, stressing the need to better understand the driving factors controlling this biogeochemical variability. Future studies in salt marshes should seek to identify so-called master variables that will allow researchers to be confident that sampling schemes capture the appropriate scales of variability such that results are representative of the entire marsh system. Given that the distance from the tidal creek explained the largest differences in our dataset, marsh hydrology is one potential master variable of interest and should be integrated into future studies. More data is needed to best identify appropriate sampling strategies for understanding the distribution of C stores in a salt marsh so we can understand and monitor climate change-induced impacts on blue C.

In both the DOC and BEPOC pools, EEMs data were suggestive of the accumulation of humified, aromatic compounds at depth. Shallow depths showed more microbial and marine influence suggestive of a more labile organic carbon pool. Despite overlap in trends, it is apparent that DOC and BEPOC have distinct compositions throughout the marsh. More data are needed to understand these carbon pools. It is important to reassess these values at different plant phenophases, tidal and depth ranges, salinities, and climatic regions to confirm the observations made here. In future work using these and more advanced analytical approaches, biogeochemists can investigate the sources and processes leading to the sequestration of blue carbon in these important coastal environments.

Acknowledgements

The author thanks the University of Delaware College of Earth, Ocean, & Environment for creating this research opportunity and the National Science Foundation REU program (Award #1757840) and American Chemical Society Petroleum Research Fund (Award #61532) for funding this project. The author also thanks Dr. Alina Ebling for training within the lab and on instruments and Tia Ouyang for her help with data coding and processing.

References

1. Mcleod, E., Chmura, G. L., Bouillon, S., Salm, R., Björk, M., Duarte, C. M., Lovelock, C. E., Schlesinger, W. H., & Silliman, B. R. *Frontiers in Ecology and the Environment*. 2011, *9*(10), 552–560.
2. Mudd, S. M., Howell, S. M., & Morris, J. T. *Estuarine, Coastal and Shelf Science*. **2009**, *82*(3), 377–389.
3. Vázquez-Lule, A., & Vargas, R. *Agricultural and Forest Meteorology*. **2021**, *300*, 108309.
4. Ding, W., Cai, Z., Tsuruta, H., & Li, X. *Chemosphere*. **2003**, *51 (3),* 167-173.
5. Moffett, K. B., & Gorelick, S. M. *Water Resources Research*. **2016**, *52*(3), 1729–1745.
6. Tucker, K. J. *Variability of organic carbon accumulation on a tidal wetland coast*. **2016**. [Thesis, University of Delaware].
7. Xiao, Y., Hoikkala, L., Kasurinen, V., et al. *JGR Biogeosciences.* **2016,** *121 (10),* 2544 - 2561.
8. Pallenbarg, R. *Estuarine, Coastal, and Shelf Science.* **1984,** *18 (3),* 331 - 346.
9. Van de Broek, M., Temmerman, S., Merckx, R., & Govers, G. *Biogeosciences.* **2016,** *13,* 6611-6624.
10. Taylor & Francis Group. *A Blue Carbon Primer.* **2018,** 27-50.
11. Van de Broek, M. & Govers, G. *Geoderma.* **2019,** *337,* 555-564.
12. Tiner, R. W., Biddle, M. A., Jacobs, A. D., Rogerson, A. B., & McGuckin, K. G. *Cooperative National Wetlands Inventory*, **2011**, 40.
13. Sharp, J. H., Benner, R., Bennett, L., Carlson, C. A., Dow,

R., & Fitzwater, S. E. *Limnology and Oceanography*. **1993**, *38*(8), 1774–1782.
14. Willey, J. D., Kieber, R. J., Eyman, M. S., & Avery, G. B. *Global Biogeochemical Cycles*. **2000**, *14*(1), 139–148.
15. McKnight, D. M., Boyer, E. W., Westerhoff, P. K., Doran, P. T., Kulbe, T., & Andersen, D. T. *Limnology and Oceanography*. **2001**, *46*(1), 38–48.
16. Lawaetz, A. J., & Stedmon, C. A. *Applied Spectroscopy*. **2009**, *63*(8), 936–940.
17. Massicotte, P. *EemR 1.0.0*. **2019**.
18. Brym, A., Paerl, H. W., Montgomery, M. T., Handsel, L. T., Ziervogel, K., & Osburn, C. L. *Marine Chemistry*. **2014**, *162*, 96–113.
19. Stookey, L. *Anal. Chem.* **1970,** *42 (7),* 779-781.
20. Xin, P., Yuan, L., Li, L., & Barry, D.A. *Water Resources Research.* **2011**, *47*(7).
21. Romigh, M.M., Davis, S.E., Rivera-Monroy, V.H., & Twilley, R. *Hydrobiologia.* **2006,** *569,* 505–516.
22. Kostka, J. & Luther III, G. *Geochim. et Cosmo.* **1994**, *58(7)*, 1701-1710.
23. Luther III, G. & Church, T. *Seasonal Cycling of Sulfur and Iron in Porewaters of a Delaware Salt Marsh.* **1987**. [University of Delaware].
24. Luther III, G., Kostka, J., Church, T., Sulzberger, B., & Stumm, W. *Marine Chem.* **1992**, *40*, 81-103.
25. Blaser, P., & Sposito, G. *Soil Science Society of America Journal*. **1987**, *51*(3), 612–619.
26. Rickard, D., & Luther III, G. *Chemistry of Iron Sulfides | Chemical Reviews*. **2007**.
27. Coble, P., Lead, J., Baker, A., Reynolds, D., & Spencer, R. G. M. *Aquatic Organic Matter Fluorescence*. **2014**, 408.
28. Lakowicz, J. R. (Ed.) *Principles of Fluorescence Spectroscopy.* **2006**, 331-351.
29. Doane, T. A., & Horwáth, W. R. *Chemosphere*. **2010**, *78*(11), 1409–1415.
30. Bowen, J. C., Clark, C. D., Keller, J. K., & De Bruyn, W. J. *Marine Pollution Bulletin*. **2017**, *114*(1), 157–168.
31. Huguet, A., Vacher, L., Relexans, S., Saubusse, S., Froidefond, J. M., & Parlanti, E. *Organic Geochemistry*. **2009**, *40*(6), 706–719.
32. Helms, J. R., Stubbins, A., Ritchie, J. D., Minor, E. C., Kieber, D. J., & Mopper, K. *Limnology and Oceanography*. **2008**, *53*(3), 955–969.